Fragmentation of and electron detachment from hot copper and silver dimer anions: A comparison

E. K. Anderson,[1,2,*] A. F. Schmidt-May,[1] P. K. Najeeb,[1] G. Eklund,[1] K. C. Chartkunchand,[3] S. Rosén,[1] M. Kamińska,[1] M. H. Stockett,[1] R. Nascimento,[4] K. Hansen,[5] Å. Larson,[1] H. Cederquist,[1] H. Zettergren,[1] and H. T. Schmidt[1,†]

[1]*Department of Physics, Stockholm University, AlbaNova, SE-106 91 Stockholm, Sweden*

[2]*Department of Physics and Astronomy, Aarhus University, DK-8000C Aarhus, Denmark*

[3]*Atomic, Optical, and Molecular Physics Laboratory, RIKEN Cluster for Pioneering Research Wako-shi, Saitama 351-0198, Japan*

[4]*Centro Federal de Educação Tecnológica Celso Suckow da Fonseca, Petrópolis, 25620-003, Rio de Janeiro, Brazil*

[5]*Center for Joint Quantum Studies and Department of Physics, School of Science, Tianjin University, 92 Weijin Road, Tianjin 300072, China*

(Received 6 March 2023; accepted 6 June 2023; published 30 June 2023)

We measured the spontaneous decays of internally hot copper and silver dimer anions, Cu_2^- and Ag_2^-, stored in one of the two ion-beam storage rings of the Double Electrostatic Ion Ring Experiment (DESIREE) at Stockholm University. A coincidence detection technique was utilized enabling essentially background-free measurements of $Cu_2^- \rightarrow Cu + Cu^-$ and $Ag_2^- \rightarrow Ag + Ag^-$ fragmentation rates. Furthermore, the total rates of neutral decay products (monomers and dimers) were measured and the relative contributions of fragmentation and electron emission ($Cu_2^- \rightarrow Cu_2 + e^-$ and $Ag_2^- \rightarrow Ag_2 + e^-$) were deduced as functions of storage time. Fragmentation is completely dominant at early times. However, after about 20 ms of storage, electron emission is observed and becomes the leading decay path after 100 ms for both dimer anions. The branching ratios between fragmentation and electron emission (vibrationally assisted autodetachment processes) are very nearly the same for Cu_2^- and Ag_2^- throughout the present storage cycle of 10 seconds. This is surprising considering the difference between the electron affinities of the neutral dimers, Cu_2 and Ag_2, and the difference between the Cu_2^- and the Ag_2^- dissociation energies.

DOI: 10.1103/PhysRevA.107.062824

I. INTRODUCTION

With the introduction of electrostatic ion-beam storage rings [1] and traps [2], the ability to store charged particle beams for extended times was combined with high-sensitivity detection of neutral particles from decay processes. For cluster ions, this has provided ideal conditions for studies of spontaneous decay processes [3]. Much of this work has been performed in room temperature devices where collisions with the residual gas (at pressures of $\sim 10^{-10}$ mbar) typically limited the time the decay can be followed to tens of milliseconds [1,4]. The development of cryogenic electrostatic ion-beam storage, where residual gas densities are reduced by orders of magnitude (to about 10^{-14} mbar or lower), has extended the times over which spontaneous decay processes can be followed to tens of seconds and beyond [5–15].

Decays following a power law have been observed for a range of cluster and molecular systems including metals, hydrocarbons, and biomolecules. This behavior has been explained with reference to broad internal energy distributions and the resulting broad distribution of thermal decay constants of the stored ions [3,11,16–18]. For large systems with many vibrational degrees of freedom one finds the quasicontinua of excitation energies for the considered ion ensembles. With strong dependencies of the decay rates on the internal energies, integration over energy then results in power-law decays [3]. However, diatomic systems have only a single vibrational degree of freedom and a power-law decay was therefore not expected by the same argument. Yet power-law decays for ensembles of stored Cu_2^- and Ag_2^- ions were observed by Fedor *et al.* using the room-temperature storage ring, ELectrostatic Ion Storage ring, Aarhus (ELISA) [19]. They found that the spontaneous neutral decay followed a $1/t$ behavior for times after ion injection up to ~8 ms and ~35 ms for the Cu_2^- and Ag_2^- anion beams, respectively. After these times, the decay deviated from the power-law behavior, and this deviation was attributed to collisions with the residual background gas. The decays were followed to 15 ms and 80 ms for Cu_2^- and Ag_2^-, respectively. Fedor *et al.* concluded, with the support of theoretical modeling, that the observed neutrals from the dimer decays were atomic fragments from dissociation processes of dimer anions in high rotational levels [19]. For dimer ions with high angular momenta, a centrifugal barrier was formed and ions with sufficient vibrational excitation were able to dissociate by tunneling through this barrier with

*eemma.anderson@gmail.com
†schmidt@fysik.su.se

decay rates depending strongly on their specific vibrational and rotational quantum numbers. As the relevant rotational quantum numbers were in the range of several hundreds, very many close-lying rovibrational levels were involved and the quasicontinuous distribution of decay rates required for the power-law behavior was realized.

In a previous experiment at the Double Electrostatic Ion Ring Experiment (DESIREE), the rate of atomic anions from fragmentation and the combined rate of neutrals from fragmentation and the electron emission of Ag_2^- were measured with two different detectors [12]. It was then found that the electron emission rate exceeded the fragmentation rate after about 100 ms of storage [12]. This was very surprising as electron emission requires a large change in the vibrational energy of the system, and no avoided curve crossings to mediate such transfer of vibrational to electronic energy were available in a Born-Oppenheimer picture. The observed electron emission [12] was described qualitatively as being due to a direct coupling of vibrational and electronic motion for dimer anions in rovibrational levels with the internal energy exceeding the electron affinity, but with insufficient rotational excitation to decay by tunneling dissociation. This general picture was supported by pioneering quantitative theoretical analyses by Jasik *et al.* [20]. Earlier decay-channel specific investigations of a similar nature are limited to a single study of Al_4^- in an electrostatic ion-beam trap [21].

Here, we report on *coincidence* measurements between Cu and Cu^- from fragmentation and measurements of Cu and Cu_2 from fragmentation and electron emission, respectively, in a separate detector. In addition, we include the corresponding results for the decay of Ag_2^- for comparison. Surprisingly, we find that the ratios between the contributions from fragmentation and electron emission are very nearly the same at all times between 200 μs and 10 s for stored ensembles of hot silver and copper dimer anions. Using the coincidence detection scheme, we directly test the assumption made in [12] and the hypothesis presented by Fedor *et al.* [19]: that the observed decay is dominated by fragmentation events for storage times up to tens of milliseconds. We present the spontaneous total neutral particle and fragmentation rates for stored ensembles of Cu_2^- and Ag_2^- ions as functions of time after their production from 200 μs to 10 s. While we confirm the complete dominance of fragmentation processes for the time range considered by Fedor *et al.* [19] for both systems, we also find that electron emission dominates at longer storage times for both Cu_2^- and Ag_2^- ions.

II. EXPERIMENTAL METHODS

The dimer anions were produced using a cesium sputter ion source known to produce highly excited ions with a broad range of internal vibrational and rotational excitations. Copper and silver cathodes were used to generate the anions of these metals, respectively. The ions were accelerated to 10 keV and a 90° bending magnet was used to mass select the dimer anions producing beams of $^{63}Cu_2^-$ or $^{107}Ag_2^-$ ions with typical currents of 100–200 pA. The dimer-anion beams were injected and stored in one of the storage rings of DESIREE [5,6]. The ions take approximately 100 microseconds to travel from the ion source to the storage ring. During this flight time

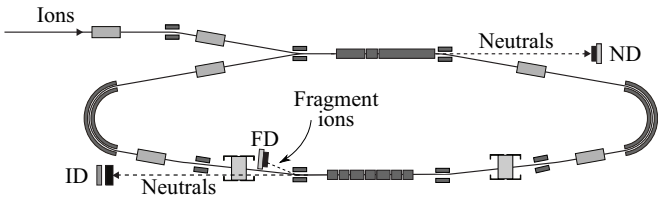

FIG. 1. A schematic of one of the DESIREE ion-beam storage rings. The imaging detector (ID) and the fragment detector (FD) are used to measure coincidences between a neutral particle (Cu or Ag) and an atomic anion (Cu^- or Ag^-) from dimer anion fragmentation events, $Cu_2^- \rightarrow Cu + Cu^-$ or $Ag_2^- \rightarrow Ag + Ag^-$. The neutral detector (ND) is used to detect neutral atoms from dimer anion fragmentation together with neutral dimers from electron emission events, $Cu_2^- \rightarrow Cu_2 + e^-$ or $Ag_2^- \rightarrow Ag_2 + e^-$ (see text).

the very hottest ions will decay, and as a result, the injected and stored anions will be vibrationally and rotationally energetic but in the electronic ground state. In Fig. 1, we show the storage ring with the detectors used in the present experiment. The detectors labeled ND (neutral detector) and FD (fragment detector) are triple-stacked microchannel-plate (MCP) detectors with resistive-anode readouts for position determinations and detection efficiencies close to the open-area ratios of the MCPs of 0.45. The detector labeled ID (imaging detector) is a triple-stack MCP with a phosphor screen anode [22] and an open-area ratio of 0.55. All three detectors register individual particle impacts, and the rates of neutrals (from ND), of atomic-ion fragments (from FD), and coincidence events (from ID and FD, see Fig. 2) are recorded up to 10 s after ion injection.

In the remainder of this section, we describe how the experiment is performed for the copper dimer anion Cu_2^-. The method is identical for the silver case. An internally hot Cu_2^- ion can decay by electron detachment or fragmentation as follows:

$$(Cu_2^-)^* \rightarrow \begin{cases} Cu^- + Cu & \text{fragmentation,} \\ Cu_2 + e^- & \text{electron detachment.} \end{cases}$$

In general, hot clusters and molecules can also decay nondestructively to stable levels through radiative cooling, as in

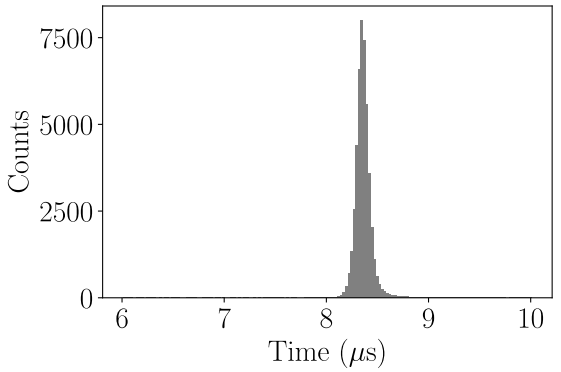

FIG. 2. A histogram of the difference in arrival times of Cu at the imaging detector (ID) and Cu^- at the FD from $Cu_2^- \rightarrow Cu + Cu^-$ fragmentation events (see text).

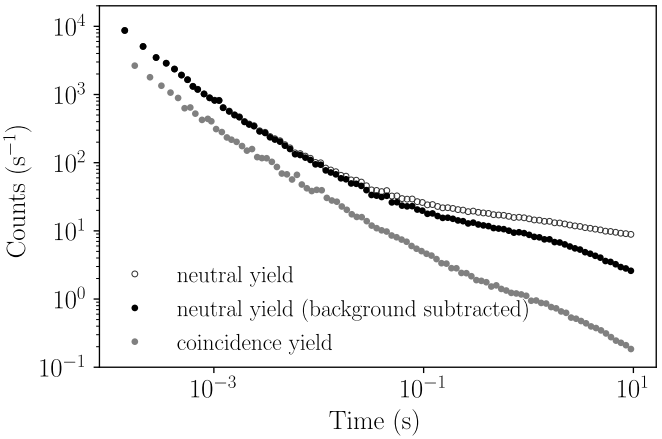

FIG. 3. Neutral yield due to electron emission and fragmentation of Cu_2^- stored in DESIREE (○), neutral yield where the detector dark count background is subtracted (●), and the coincidence yield (●) up to 10 seconds of storage (see text).

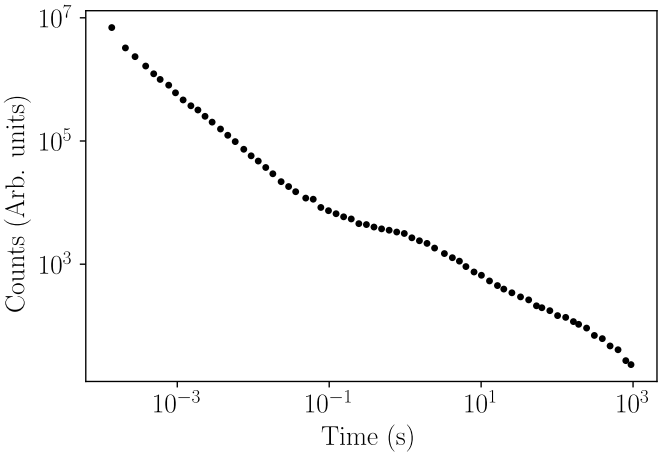

FIG. 4. Neutral yield due to electron emission and fragmentation of Cu_2^- stored in DESIREE for up to 1000 s. The fact that the signal follows a power law in the range 10 s to 1000 s indicates that only at times of the order of the ∼ 1000 s storage lifetime do residual-gas collisions affect the signal.

the case of, e.g., OH^- [23,24]. However, the homonuclear dimer systems considered here are infrared inactive as their electric dipole moment is zero, and the timescale for their radiative decay is therefore much longer than the DESIREE ion-beam storage times, even if these can exceed 1000 seconds [9,25].

When an excited copper dimer anion decays via either electron detachment or fragmentation in a straight section of the ring, those events can be detected as either a neutral dimer or as a neutral and a negatively charged monomer leaving the ring, as can be seen in Fig. 1. Neutral particles (Cu_2 from detachment events and Cu from fragmentation events) continue to travel in straightline paths and may be detected by either one of the two neutral-particle detectors (ID and ND in Fig. 1). After one of the two straight sections, a Cu^- fragment will leave the straight section with two times the angle of that of a circulating Cu_2^- ion and can thus be detected by the FD. By measuring the time intervals between detection events of the FD and ID, we can form a histogram as shown in Fig. 2 and identify the coincidences resulting from fragmentation events taking place in the preceding straight section.

For the measurements with the ND, in Fig. 1, we have background contributions from detector dark counts (about 6 s^{-1}) [6]. This dark count rate is measured without the beam before each injection and subtracted from the measured neutral yields with the beam as indicated in Fig. 3. For the coincidence measurement, the time difference between the arrival of atomic anion on the FD and the neutral atom at the ID is well defined as can be seen in Fig. 2, and the effective background for the coincidence signal is negligible.

The data shown in Figs. 3 to 5 are plotted as functions of the time after ion production using a logarithmic timescale. In order for the data points to be equidistant on this scale, the time-bin size is increased linearly with time except for the first few data points where each point corresponds to a single revolution of the ions in the storage ring.

III. RESULTS

The measured count rates of neutral particles on the ND for a stored 10 keV $^{63}Cu_2^-$ ion beam are shown in Fig. 3, before (open circles) and after (black filled circles) subtraction of the detector dark-count rate. Also shown is the rate of coincidence detection events between the FD and ID (gray filled circles).

Comparing the background-subtracted neutral rate and the rate of coincidences, we see that these two curves are parallel for the first ∼20 ms, separated by a constant factor of approximately 2. This is consistent with earlier findings for silver dimer anions [12] and with the analysis of Fedor *et al.* who concluded from their combined experimental and theoretical study [19] that the decay for early times is dominated by fragmentation through a rotational barrier. The approximate factor of 2 difference is to be expected as the coincidence rate will rely on the product of the efficiencies of both involved detectors, which both are given by the open-area ratios and close to one half.

After about 20 ms of storage, the two curves cease to be parallel and the background-corrected rate of neutrals has an additional contribution. This we ascribe to electron detachment processes for which the only product detectable (within our experimental configuration) is the neutral dimer. Interestingly, the coincidence signal due to fragmentation events also exceeds that which would follow from a continuation of the initial power-law decay at around the same time, albeit to a much smaller extent than for the neutral signal.

Fedor *et al.* [19] observed an even stronger deviation from power-law behavior after 20 ms and ascribed that to the residual-gas collisional background. However, the similar but smaller deviations from power-law decays observed here cannot be caused by such residual gas collision effects. We conclude this from Fig. 4 where the neutral rate upon storage of Cu_2^- is shown for a much longer storage time of 1000 s. When we consider the rate at long times, the signal follows a power law from about 1 s onwards and begins to decline after several hundred seconds due to the finite storage lifetime of

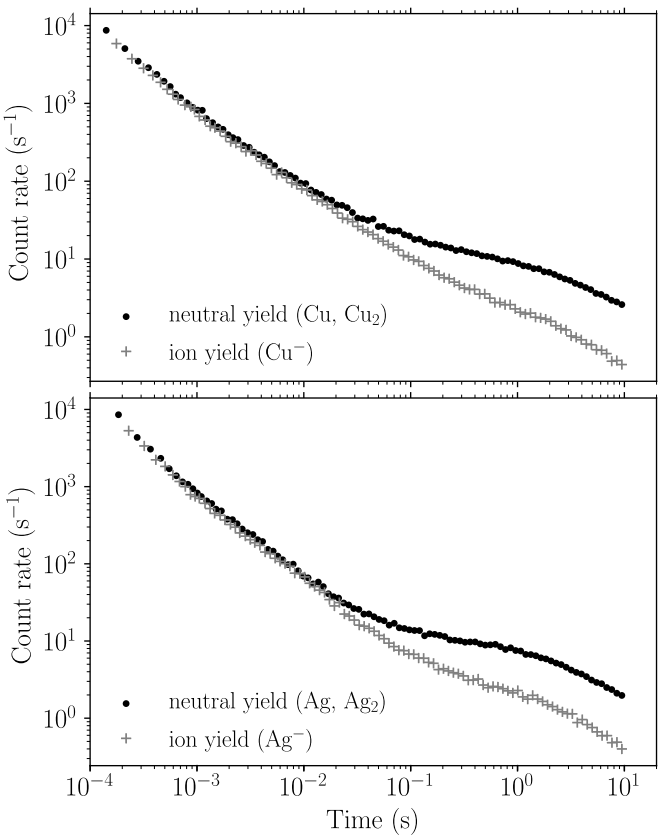

FIG. 5. Upper panel: Data recorded with stored beam of 10 keV Cu_2^-. Background-corrected count rates of neutral products (•) and ionic Cu^- fragments (+) as function of time after injection. Lower panel: Data recorded with stored beam of 10 keV Ag_2^-. Background-corrected count rates of neutral products (•) and ionic Ag^- fragments (+) as function of time after injection.

the beam, which is on the order of 1000 s. A signal dominated by residual-gas collisions would follow the exponential decay of the ion beam and not a power law. Thus, any effects of residual-gas collisions are small for this set of data and completely negligible for the data shown in Fig. 3, which extend up to 10 s only.

For the following discussion, it is important to keep in mind that, due to the fact that the symmetric dimer anions are infrared inactive, the time dependencies of the signals observed are ascribed exclusively to *depletion* of different

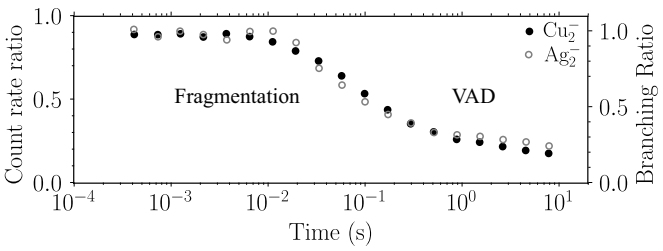

FIG. 6. The ratio of the fragment signal to the neutral signal for Cu_2^- (•) and Ag_2^- (○) stored in DESIREE. The y axis to the right shows the branching ratio for fragmentation with the assumed effective detector efficiencies (see text).

TABLE I. The literature values [26–28] for the dimer species which were used to calculate the Morse potentials presented in Figs. 7 and 8 where r_0 is the equilibrium bond length, D_0 the dissociation energy, ω_0 the vibrational frequency, and EA the electron affinity.

	r_0 (Å)	D_0 (eV)	ω_0 (cm^{-1})	EA (eV)
Cu_2	2.2197	2.02 ± 0.08	266.43	0.836 ± 0.007
Cu_2^-	2.343 ± 0.007	1.62 ± 0.20	196 ± 15	–
Ag_2	2.480	1.65 ± 0.03	192.4	1.023 ± 0.007
Ag_2^-	2.604 ± 0.007	1.37 ± 0.16	145 ± 10	–

classes of rovibrational levels with very different decay rates rather than to internal cooling processes.

To establish a quantitative measure of the relative contributions of the fragmentation and electron emission processes, we display (in Fig. 5 upper panel) the background-corrected count rates on the FD and ND for stored copper dimer anions. In the lower panel of Fig. 5, we show the corresponding data for silver dimer anions. We note that fragmentation will contribute to the signals on both detectors while electron emission will only contribute to the ND signal. Thus, for equal detection efficiencies, the fraction of all decays that are due to fragmentation is given directly by the ratio of the signal on the FD to that on the ND after background subtractions. These signal ratios are shown in Fig. 6.

As the electron detachment process is only identified indirectly as the differences in count rates of the two detectors, we carefully investigate if time-dependent systematic effects possibly could affect the measured decays. The detectors are position-sensitive so we can exclude any drift of the beam, as this would lead to different positions of the singly charged atomic anions from fragmentation events after different times of storage. No such drifts were observed. In addition, measurements were repeated with very different beam currents to exclude any saturation or recovery effects that could result in deviations of the efficiencies of the two detectors.

We find for copper and silver dimer anions alike that the measured signal ratios are constant at around 0.9 until about 20 ms after injection, when they start to decrease significantly. The effective detection efficiencies are not precisely known and the found constant value is thus consistent with effectively 100% fragmentation for this early part of the decay and a factor of 0.9 between the detection efficiencies for the FD and ND. The measured branching ratios for fragmentation are then given by the right-hand vertical axis in Fig. 6. We find that the relative contribution from electron emission becomes detectable at about $t = 10$ ms and then increases with time to reach approximately 75% for several seconds of storage. It is quite remarkable that this behavior is close to identical for the copper and silver dimer anions studied in view of the very different values of dimer electron affinities and dimer ion dissociation energies of the two systems (see Table I).

IV. DISCUSSION

As discussed above, the early decay was ascribed by Fedor *et al.* [19] to the fragmentation of dimer anions in very highly

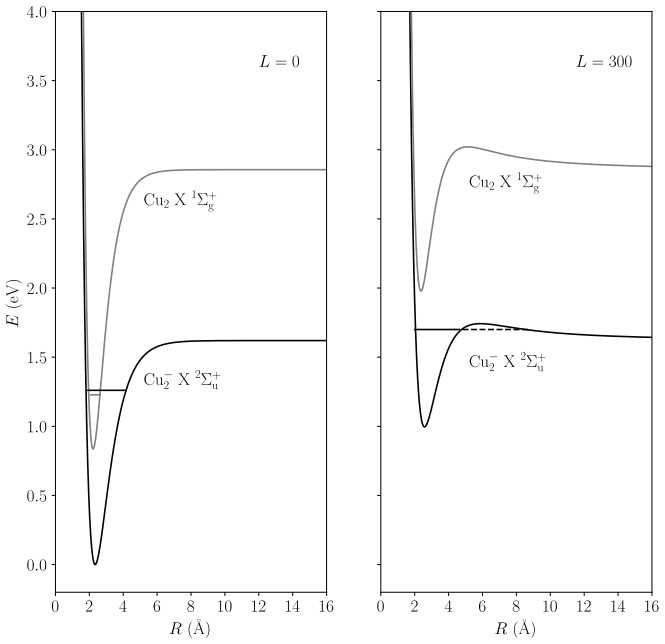

FIG. 7. Morse potentials for copper dimer anions and neutral dimers for low ($L = 0$) and high ($L = 300$) rotations. The vibrational levels are included as illustrative examples and are $v = 52$ for the $L = 300$ level that decays by tunneling fragmentation and $v = 70$ for the nonrotating dimer anion that decays by electron emission to the $v = 12$ vibrational level of the neutral dimer. The vibrational level structures are calculated by numerically solving the Schrödinger equations for the nuclear motion in the given potentials (see text).

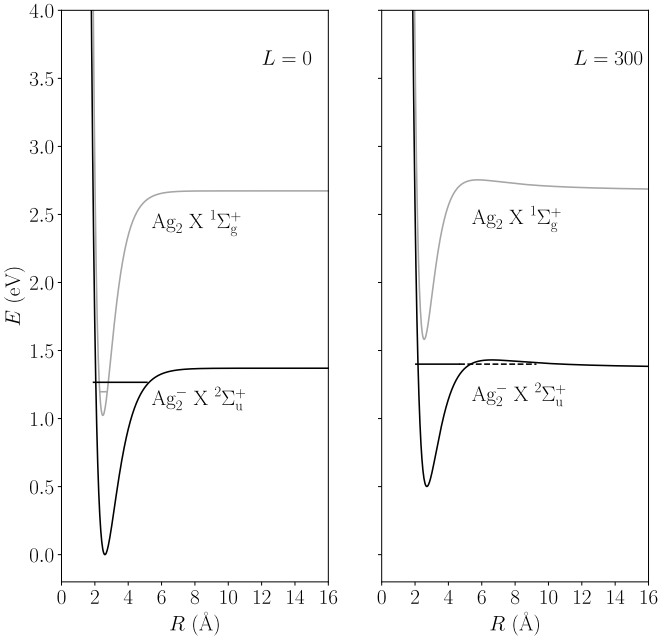

FIG. 8. Morse potentials for silver dimer anions and neutral dimers for low ($L = 0$) and high ($L = 300$) rotations. The vibrational levels are included as illustrative examples and are $v = 88$ for the $L = 300$ level that decays by tunneling fragmentation and $v = 110$ for the nonrotating dimer anion that decays by electron emission to the $v = 7$ vibrational level of the neutral dimer. The vibrational level structures are calculated by solving the Schrödinger equations for the nuclear motion in the given potentials (see text).

excited rotational levels by tunneling through the rotational barrier. For less highly excited rotational levels, this decay path is not available. Given that the electron affinities for both Cu_2 and Ag_2 are smaller than the fragmentation energies of the respective dimer anions (see Table I), dimer anions with low *rotational* but high *vibrational* excitations are stable against fragmentation but energetically allowed to decay via vibrational autodetachment (VAD) processes to neutral dimers with similar rotational excitation but much reduced vibrational quantum numbers. We thus ascribe the observation at longer times of neutral dimers to VAD processes undergone by dimer anions with insufficient rotational excitation for the tunneling process originally suggested by Fedor *et al.* to take place, but sufficient *vibrational* excitation to exceed the electron affinity. We further note that the high rate of neutrals from fragmentation prohibits the observation of this process at early times, both in this work and in previous studies [19]. For the case of silver dimer anions this interpretation was provided in Ref. [12] and supported by subsequent quantitative theoretical work by Jasik *et al.* [20].

The fragmentation and electron emission processes are illustrated by the approximate potential energy curves for copper and silver dimers and dimer anions shown in Figs. 7 and 8, respectively. The curves are Morse potentials based on the parameters given in Table I taken from Refs. [26–28]. The left panels show the potential energy curves for nonrotating systems while the right panels show the curves resulting when the centrifugal distortions with $L = 300$ are added.

The right panels of Figs. 7 and 8 display examples of rovibrational levels, which can dissociate by tunneling through the centrifugal barriers as discussed by Fedor *et al.* [19] and (for silver dimer anions only) by Anderson *et al.* [12] and Jasik *et al.* [20]. In the left panels single dimer anion $L = 0$ vibrational levels are shown as well as single vibrational levels of the neutral dimer. This serves to illustrate the energetically possible decays where electrons, with kinetic energies given as the difference energies of these anion and neutral levels, are emitted.

The vibrational energies are calculated for each of the potentials shown in Figs. 7 and 8 by solving the Schrödinger equation numerically as discussed for the case of silver in Ref. [12]. Such numerical calculations are performed for neutral and anion dimers of silver and copper for all angular momenta L for which any bound states exist for the nuclear motion. Ignoring the angular momentum carried by any emitted electron, the rovibrational levels are sorted according to their energetically possible decay modes as illustrated in Figs. 9 and 10 for the copper and silver cases, respectively. The anion levels of Figs. 7 and 8 are indicated in Figs. 9 and 10 by the filled circles and triangles for the $L = 0$ and $L = 300$ cases.

While the details of the two maps shown in Figs. 9 and 10 are different, their qualitative features are strikingly similar. Both Cu_2^- and Ag_2^- are stable systems and obviously no spontaneous electron emission or fragmentation can occur for low rotational and vibrational excitations. For low L we see that electron emission becomes possible with sufficient vibrational

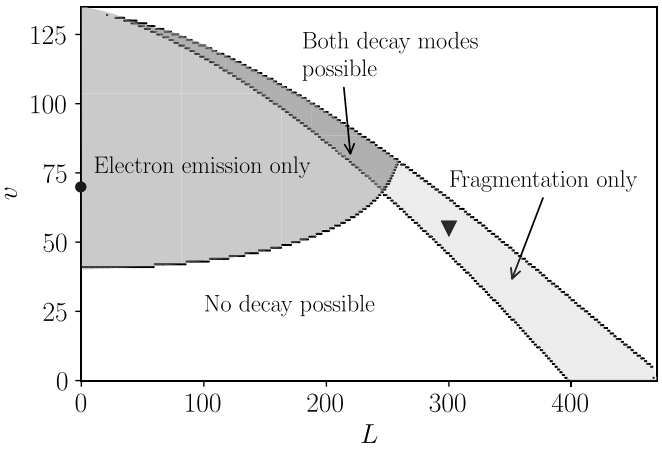

FIG. 9. Map of rovibrational levels of Cu_2^- indicating which levels are stable and which can decay by fragmentation and/or electron emission. The filled circle and triangle indicate the anion levels shown in the left and right panels of Fig. 7, respectively.

excitation as also indicated in the left panels of Figs. 7 and 8. With increasing values of L, metastable rovibrational levels form behind the centrifugal barrier and fragmentation by tunneling through that barrier become a possible decay path. We further note that for certain areas of these rovibrational maps both decay paths are open, but also that there is a higher limit of L beyond which electron emission is no longer possible. Inspecting Figs. 7 or 8 this can be understood as the neutral potential energy curve no longer "dipping" down into the part of the anion potential holding bound vibrational levels. We find the maximum L values for electron emission to be $L_{\max}^{\mathrm{Cu}} = 258$ and $L_{\max}^{\mathrm{Ag}} = 249$. In the case of silver dimer anions, Jasik *et al.* [20] performed coupled-cluster calculations including core-valence correlation to determine the potential-energy curves. They found an upper limit to L for which electron emission is possible; $L_{\max}^{\mathrm{Ag}} = 253$. This is a very small deviation from that of our simpler treatment and, as pointed out by Jasik *et al.* [20], the observed differences of

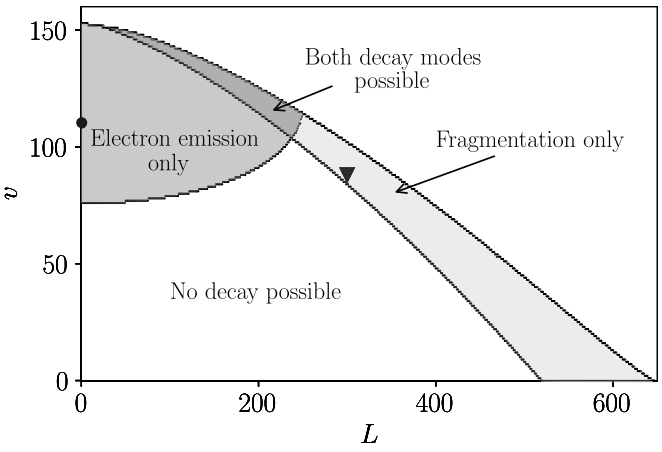

FIG. 10. Map of rovibrational levels of Ag_2^- indicating which levels are stable and which can decay by fragmentation and/or electron emission. The filled circle and triangle indicate the anion levels shown in the left and right panels of Fig. 8, respectively.

their calculated potentials compared to our Morse potentials are not expected to qualitatively alter the interpretation of the experimental data.

The specific distribution on rovibrational levels among the ions produced in the violent sputtering process is not known, but we can still get a qualitative understanding of the observed time dependence of the relative contributions of the two decay channels from the rovibrational maps shown in Figs. 9 and 10. First, we note that both dimer anions are stable for quite high rotational and/or vibrational excitations, so that the mere observation of spontaneous decays implies that very high excitations do occur. The observation that fragmentation dominates initially then implies that the region in this rovibrational map that dominates the decay is in the "Fragmentation only" part. With time the initially dominating region is depleted in favor of more slowly decaying rovibrational levels. The fact that for both systems the fraction of electron emission of the total decay rate becomes constant after a few hundred ms we interpret as the dominating region for longer times is in the part of the maps where both decays are possible. The observation that also the fragmentation signal deviates from the initial power-law dependence for longer times is then also explained by the slower decay of these vibrational levels.

The fragmentation processes dominating the signals up to about 100 ms after injection can be understood as quantum mechanical tunneling through the centrifugal barrier [19,20]. Concerning electron emission, which for both systems dominate for longer times, the mechanism is less intuitive. Quantum mechanically, the transition of the electron from a state of the anion to a continuum state relies on nonadiabatic couplings. In a strict Born-Oppenheimer approach such nonadiabatic couplings are zero, but when the anion and neutral potentials are close (at avoided crossings) they can be significant. Here, the neutral and anionic curves do not cross and the nonadiabatic couplings are weak although not vanishing. This was expressed formally in Anderson *et al.* [12], and Jasik *et al.* [20] calculated the rates for electron emission from silver dimer anions in a large number of rovibrational levels. They found rates as low as 0.1 s^{-1}, consistent with the observation of this process 10 s after ion injection.

The importance of (the absence of any) curve crossings can be understood in a time-dependent picture. Assume that the potential energy curves of the anion and neutral states would actually cross. Then an electron-emission process would take place at the moment when the nuclear motion in the anionic initial state passes the internuclear distance where the anionic curve crosses that of the neutral (shifted upward by a small amount to account for the kinetic energy of the emitted electron). This upward-shifted curve would represent the system of neutral plus free electron and would have an avoided crossing with the anionic state. Hence, on the first passage in the vibrational motion, the system can follow the adiabatic curve and an electron emission will result where the vibrational excitation changes on the timescale of a vibrational period. This would not require any sudden change in the internuclear distance or its time derivative. On the other hand, an electron emission in the *absence* of such a crossing implies a sudden change in the relative motion of the nuclei through a direct exchange of momentum between the nuclear and electronic degrees of freedom. A very unlikely process and explicitly

at odds with the basic assumptions of the Born-Oppenheimer approach.

This important distinction between weak and strong adiabatic couplings was also discussed by Jasik *et al.* [20]. In their Introduction, they discussed the present case of very weak nonadiabatic couplings and the need for long-time storage in devices like DESIREE in contrast to cases with strong coupling and rapid processes, which are studied experimentally with ultrafast lasers.

V. CONCLUSION

In a recent Letter [12], decays by electron emission were identified for internally hot silver dimer anions and ascribed to very slow vibrational autodetachment in the absence of any avoided crossings of adiabatic potential energy curves. This interpretation is supported by recent theoretical results for silver dimer anions [20]. Here, we present results for the decay of hot copper dimer anions and find, as in the case of silver, that fragmentation dominates initially while electron emission takes over as the dominating decay at around 100 ms for Cu_2^- and Ag_2^- alike. When comparing the relevant potential energy curves for the two cases, it is not surprising that the decays exhibit similar types of features. It is, however, remarkable that the ratios of the two decay mechanisms as functions of time from 100 μs to 10 s are *close to identical* for the two systems, considering their quite different values of dimer electron affinities and dimer anion dissociation energies. To shed more light on this surprising result, we plan additional experiments with other homonuclear dimers with different energetic properties (electron affinities and dimer anion dissociation energies) to see if this changes the balance between the two decay modes.

All resulting data shown in the figures are available electronically under a Creative Commons license [29].

ACKNOWLEDGMENTS

This work was performed at the Swedish National Infrastructure, DESIREE (Swedish Research Council Contracts No. 2017-00621 and No. 2021-00155). Furthermore, A.F.S.-M., M.H.S., Å.L., H.C., H.Z., and H.T.S. acknowledge the project grant "Probing charge- and mass- transfer reactions on the atomic level" (Grant No. 2018.0028) from the Knut and Alice Wallenberg Foundation. Finally, H.C., H.Z., and H.S. thank the Swedish Research Council for their project grants (Contracts No. 2019-04379, No. 2020-03437, and No. 2022-02822).

[1] S. P. Møller, Elisa, an electrostatic storage ring for atomic physics, Nucl. Instrum. Methods Phys. Res., Sect. A **394**, 281 (1997).

[2] D. Zajfman, O. Heber, L. Vejby-Christensen, I. Ben-Itzhak, M. Rappaport, R. Fishman, and M. Dahan, Electrostatic bottle for long-time storage of fast ion beams, Phys. Rev. A **55**, R1577(R) (1997).

[3] K. Hansen, J. U. Andersen, P. Hvelplund, S. P. Møller, U. V. Pedersen, and V. V. Petrunin, Observation of a $1/t$ Decay Law for Hot Clusters and Molecules in a Storage Ring, Phys. Rev. Lett. **87**, 123401 (2001).

[4] S. Jinno, T. Takao, Y. Omata, A. Satou, H. Tanuma, T. Azuma, H. Shiromaru, K. Okuno, N. Kobayashi, and I. Watanabe, TMU electrostatic ion storage ring designed for operation at liquid nitrogen temperature, Nucl. Instrum. Methods Phys. Res., Sect. A **532**, 477 (2004).

[5] R. D. Thomas, H. T. Schmidt, G. Andler, M. Björkhage, M. Blom, L. Brännholm, E. Bäckström, H. Danared, S. Das, N. Haag *et al.*, The double electrostatic ion ring experiment: A unique cryogenic electrostatic storage ring for merged ion-beams studies, Rev. Sci. Instrum. **82**, 065112 (2011).

[6] H. T. Schmidt, R. D. Thomas, M. Gatchell, S. Rosén, P. Reinhed, P. Löfgren, L. Brännholm, M. Blom, M. Björkhage, E. Bäckström *et al.*, First storage of ion beams in the double electrostatic ion-ring experiment: DESIREE, Rev. Sci. Instrum. **84**, 055115 (2013).

[7] R. von Hahn, A. Becker, F. Berg, K. Blaum, C. Breitenfeldt, H. Fadil, F. Fellenberger, M. Froese, S. George, J. Göck *et al.*, The cryogenic storage ring CSR, Rev. Sci. Instrum. **87**, 063115 (2016).

[8] M. Lange, M. Froese, S. Menk, J. Varju, R. Bastert, K. Blaum, J. R. C. López-Urrutia, F. Fellenberger, M. Grieser, R. von Hahn *et al.*, A cryogenic electrostatic trap for long-time storage of keV ion beams, Rev. Sci. Instrum. **81**, 055105 (2010).

[9] E. Bäckström, D. Hanstorp, O. M. Hole, M. Kaminska, R. F. Nascimento, M. Blom, M. Björkhage, A. Källberg, P. Löfgren, P. Reinhed, S. Rosén, A. Simonsson, R. D. Thomas, S. Mannervik, H. T. Schmidt, and H. Cederquist, Storing Kev Negative Ions for an Hour: The Lifetime of the Metastable $^2P^o_{1/2}$ Level in $^{32}S^-$, Phys. Rev. Lett. **114**, 143003 (2015).

[10] K. Hansen, M. H. Stockett, M. Kaminska, R. F. Nascimento, E. K. Anderson, M. Gatchell, K. C. Chartkunchand, G. Eklund, H. Zettergren, H. T. Schmidt, and H. Cederquist, Spontaneous decay of small copper-cluster anions Cu_n^- ($n = 3 - 6$), on long time scales, Phys. Rev. A **95**, 022511 (2017).

[11] E. K. Anderson, M. Kamińska, K. C. Chartkunchand, G. Eklund, M. Gatchell, K. Hansen, H. Zettergren, H. Cederquist, and H. T. Schmidt, Decays of excited silver-cluster anions Ag_n, $n = 4$ to 7, in the Double ElectroStatic Ion Ring ExpEriment, Phys. Rev. A **98**, 022705 (2018).

[12] E. K. Anderson, A. F. Schmidt-May, P. K. Najeeb, G. Eklund, K. C. Chartkunchand, S. Rosén, A. Larson, K. Hansen, H. Cederquist, H. Zettergren, and H. T. Schmidt, Spontaneous Electron Emission from Hot Silver Dimer Anions: Breakdown of the Born-Oppenheimer Approximation, Phys. Rev. Lett. **124**, 173001 (2020).

[13] M. Gatchell, J. Ameixa, M. Ji, M. H. Stockett, A. Simonsson, S. Denifl, H. Cederquist, H. T. Schmidt, and H. Zettergren, Survival of polycyclic aromatic hydrocarbon knockout fragments in the interstellar medium, Nat. Commun. **12**, 6646 (2021).

[14] M. H. Stockett, J. N. Bull, H. T. Schmidt, and H. Zettergren, Statistical vibrational autodetachment and radiative cooling rates of para-benzoquinone, Phys. Chem. Chem. Phys. **24**, 12002 (2022).

[15] C. Breitenfeldt, K. Blaum, M. W. Froese, S. George, G. Guzmán-Ramírez, M. Lange, S. Menk, L. Schweikhard, and A. Wolf, Decay processes and radiative cooling of small anionic copper clusters, Phys. Rev. A **94**, 033407 (2016).

[16] M. Goto, A. E. K. Sundén, H. Shiromaru, J. Matsumoto, H. Tanuma, T. Azuma, and K. Hansen, Direct observation of internal energy distributions of C_5^-, J. Chem. Phys. **139**, 054306 (2013).

[17] J. U. Andersen, H. Cederquist, J. S. Forster, B. A. Huber, P. Hvelplund, J. Jensen, B. Liu, B. Manil, L. Maunoury, S. Brøndsted Nielsen, U. V. Pedersen, H. T. Schmidt, S. Tomita, and H. Zettergren, Power-law decay of collisionally excited amino acids and quenching by radiative cooling, Eur. Phys. J. D **25**, 139 (2003).

[18] S. Martin, J. Bernard, R. Brédy, B. Concina, C. Joblin, M. Ji, C. Ortega, and L. Chen, Fast Radiative Cooling of Anthracene Observed in a Compact Electrostatic Storage Ring, Phys. Rev. Lett. **110**, 063003 (2013).

[19] J. Fedor, K. Hansen, J. U. Andersen, and P. Hvelplund, Non-thermal Power Law Decay of Metal Dimer Anions, Phys. Rev. Lett. **94**, 113201 (2005).

[20] P. Jasik, J. Franz, D. Kedziera, T. Kilich, J. Kozicki, and J. E. Sienkiewicz, Spontaneous electron emission vs dissociation in internally hot silver dimer anions, J. Chem. Phys. **154**, 164301 (2021).

[21] B. Kafle, O. Aviv, V. Chandrasekaran, O. Heber, M. L. Rappaport, H. Rubinstein, D. Schwalm, D. Strasser, and D. Zajfman, Electron detachment and fragmentation of laser-excited rotationally hot Al_4^-, Phys. Rev. A **92**, 052503 (2015).

[22] S. Rosén, H. T. Schmidt, P. Reinhed, D. Fischer, R. D. Thomas, H. Cederquist, L. Liljeby, L. Bagge, S. Leontein, and M. Blom, Operating a triple stack microchannel plate-phosphor assembly for single particle counting in the 12-300 K temperature range, Rev. Sci. Instrum. **78**, 113301 (2007).

[23] H. T. Schmidt, G. Eklund, K. C. Chartkunchand, E. K. Anderson, M. Kamińska, N. de Ruette, R. D. Thomas, M. K. Kristiansson, M. Gatchell, P. Reinhed, S. Rosén, A. Simonsson, A. Källberg, P. Löfgren, S. Mannervik, H. Zettergren, and H. Cederquist, Rotationally Cold OH^- Ions in the Cryogenic Electrostatic Ion-Beam Storage Ring Desiree, Phys. Rev. Lett. **119**, 073001 (2017).

[24] C. Meyer, A. Becker, K. Blaum, C. Breitenfeldt, S. George, J. Göck, M. Grieser, F. Grussie, E. A. Guerin, R. von Hahn *et al.*, Radiative Rotational Lifetimes and State-Resolved Relative Detachment Cross Sections from Photodetachment Thermometry of Molecular Anions in a Cryogenic Storage Ring, Phys. Rev. Lett. **119**, 023202 (2017).

[25] M. K. Kristiansson, S. Schiffmann, J. Grumer, J. Karls, N. de Ruette, G. Eklund, V. Ideböhn, N. D. Gibson, T. Brage, H. Zettergren, D. Hanstorp, and H. T. Schmidt, Experimental and theoretical studies of excited states in Ir^-, Phys. Rev. A **103**, 062806 (2021).

[26] J. Ho, K. M. Ervin, and W. C. Lineberger, Photoelectron spectroscopy of metal cluster anions: Cu_n^-, Ag_n^-, and Au_n^-, J. Chem. Phys. **93**, 6987 (1990).

[27] M. D. Morse, Clusters of transition-metal atoms, Chem. Rev. **86**, 1049 (1986).

[28] L. D. Socaciu-Siebert, J. Hagen, J. Le Roux, D. Popolan, M. Vaida, Š. Vajda, T. M. Bernhardt, and L. Wöste, Ultrafast nuclear dynamics induced by photodetachment of Ag_2^- and $Ag_2O_2^-$: Oxygen desorption from a molecular silver surface, Phys. Chem. Chem. Phys. **7**, 2706 (2005).

[29] The data are available at the following repository, DOI:10.5281/zenodo.7664520.